ISSN 0036-0295, Russian Metallurgy (Metally), Vol. 2015, No. 1, pp. 36–42. © Pleiades Publishing, Ltd., 2015.
Original Russian Text © V.N. Serebryany, V.Yu. Perezhogin, G.I. Raab, V.I. Kopylov, N.Yu. Tabachkova, V.P. Sirotinkin, S.V. Dobatkin, 2015, published in Metally, 2015, No. 1, pp. 42–49.

Structure, Texture, and Mechanical Properties of an MA2-1hp Magnesium Alloy after Two-Stage Equal-Channel Angular Pressing and Intermediate Annealing

V. N. Serebryany[a], V. Yu. Perezhogin[b], G. I. Raab[c], V. I. Kopylov[d], N. Yu. Tabachkova[b], V. P. Sirotinkin[a], and S. V. Dobatkin[a, b]

[a] *Baikov Institute of Metallurgy and Materials Science, Russian Academy of Sciences, Moscow, 119991 Russia*
e-mail: vns@imet.ac.ru
[b] *National University of Science and Technology MISiS, Moscow, 119049 Russia*
[c] *Institute of Physics of Advanced Materials, Ufa State Aviation Technical University, Ufa, 450000 Russia*
[d] *Physical-Technical Institute, National Academy of Sciences of Belarus, Minsk, Belarus*

Received March 11, 2014

Abstract—The effect of two-stage equal-channel angular pressing (ECAP) on the microstructure, the texture, and the mechanical properties of an MA2-1hp magnesium alloy is analyzed. ECAP leads to the formation of a submicrocrystalline structure with an average grain size of 640 nm, which includes $Mg_{17}Al_{12}$ phase particles with an average grain size of 240 nm and a volume fracture of 5.5%. A scattered tilted basal texture forms after ECAP, and its experimental pole figures are used for calculating orientation distribution functions and determining the volume fractions of the main orientations and the Schmid factors for different deformation systems. An increased activation of basal slip is found after both the first and the second stages of ECAP. As a result of two-stage ECAP, the strength properties of the alloy that correspond to the minimum acceptable values achieved by direct compression are obtained. Ductility is 44 and 18% after the first stage of ECAP plus subsequent annealing and after the second stage, respectively, which is almost four and two times higher than the initial value. The resulting strength mechanical properties of the alloy after the first and the second ECAP stages are analyzed using the Hall–Petch relation.

DOI: 10.1134/S0036029515010103

INTRODUCTION

Grain refinement and the formation of an tilted scattered basal texture in magnesium alloys during equal-channel angular pressing (ECAP) at temperatures of 200–250°C favors a noticeable increase in their ductility at a slight increase in the strength properties [1–7]. The softening effect of texture leads to almost complete neutralization of the hardening effect produced by grain refinement to 2–3 μm in these alloys. To enhance the strength properties of magnesium alloys noticeably, it is necessary to form a fine-grained structure on a submicrocrystalline level [8]. However, it is extremely difficult to do this in magnesium alloys in several passes of ECAP due to the low ductility of the alloys at pressing temperatures below 200°C. Two-stage ECAP of magnesium alloys with intermediate annealing brings this possibility to life, since the ductility of the alloys after the first stage of ECAP and subsequent annealing increases due to the formation of a scattered tilted basal texture and larger grains (~10 μm); and the achieved enhanced ductility is used at the second stage of ECAP performed in several passes when the deformation temperature is decreased continuously in each pass [8]. The formation of a submicrocrystalline structure in magnesium alloys can be achieved by varying the ECAP parameters, such as the temperature, the pressing rate, the angle of channel intersection, the number of passes, and the pressing route, at the second stage [8].

In this paper we used a two-stage ECAP scheme to form a submicrocrystalline structure in an MA2-1hp magnesium alloy to improve its mechanical properties at an increased retained ductility.

EXPERIMENTAL

The material under study was an extruded rod 80 × 90 mm in section made of an MA2-1hp alloy of the following composition (wt %): 4.4% Al, 0.9% Zn, 0.4% Mn, and Mg for balance. Samples 20 × 20 × 100 mm in dimensions cut from the rod were subjected to ECAP in two stages.

The first stage is intended for a special preparation of an alloy structure and texture, which yields the maximum ductility of the material. ECAP at this

stage occurs at an angle of channel intersection of 90° and a strain rate of 0.4 mm/s by route 2*C* (two passes at 245°C) for an investigation of the possible enhancement of the low-temperature ductility of the alloys due to microstructure refinement and texture change. In order to check the effect of the grain size and a changed texture on the ductility of the alloys, the samples after ECAP were annealed at 375°C for 1 h.

The second stage was intended for searching for the ways to improve the strength properties at a sufficiently high retained ductility. To solve this task, we made a number of additional changes during ECAP: we reduced the pressing rate, increased the angle of channel intersection to 120°, and used multipass pressing by various routes when decreasing the pressing temperature gradually from pass to pass. The following scheme of pressing was applied: after the first stage, a workpiece was subjected to ECAP at an angle of 120° between the channels and a strain rate of 0.25 mm/s in 12 passes. The first four passes of them were performed by routes *A*, *C*, *C* and B_c at a temperature of 220°C. The next four passes were carried out by the same routes at 180°C, which were followed by two passes by routes *C* and B_c at 160°C. The final two passes were performed by routes *C* and B_c at 150°C.

The rod after two-stage ECAP was used to cut samples parallel to plane *x* for microstructural and texture examination and parallel to plane *y* for measuring the tensile mechanical properties of the alloy. Metallographic sections were prepared by grinding, polishing, and etching. A sandpaper of several grades, whose grain size decreased sequentially, was used for grinding. The direction of grinding was changed by 90° when the sandpaper number was changed to the next one. Grinding was carried out until all scratches formed during the previous operation were completely removed. To remove small scratches retained after grinding and to obtain a smooth mirror section surface, polishing was performed on a polishing wheel, which was followed by chemical etching in a solution of 4.2 g picric acid, 10 mL acetic acid, 70 mL ethanol, and 10 mL water. A sample microstructure was examined using a Buehler optical microscope. The Image Expert 3.3 software was used for analyzing structure images and for building grain size distribution diagrams.

Thin foils for structure examination by transmission electron microscopy (TEM) were prepared by ion polishing with a Gatan unit. 3-mm disks were cut from initial plate-shaped samples 200 μm thick. Then, the samples were thinned by ion polishing on a PIPS installation (Precision Ion Polishing System, Gatan). For structural investigations, a JEOL JEM 2100 (Japan) transmission electron microscope with a high resolution was utilized. A JEM 2100 microscope with a point and linear resolution of 2.3 and 1.4 Å, respectively, and a maximum acceleration voltage of 200 kV has a direct magnification to 1.5 million times. A LaB_6 boride cathode was used as an electron source.

X-ray diffraction analysis (XRD) of the plate-shaped samples was carried out on a Rigaku Ultima IV (Japan) X-ray diffractometer. X-ray diffraction spectra were recorded under the same conditions: Cu$K\alpha$ radiation (Ni filter), registration of a reflected beam performed on a D/teX high-speed detector in the mode reducing the fluorescence from iron radiation, a tube voltage of 40 kV, a tube current of 30 mA, and a detector speed of 2 deg/min (1 deg/min for a small sample) on the 2θ scale at a step of 0.02°. XRD analysis was carried out using the Rigaku PDXL software, which includes the PDF-2 X-ray database. The amount of phases was determined using a PDXL package subprogram (applying the method of corundum numbers).

Texture in the form of five incomplete {10.2}, {11.0}, {10.3}, {00.4}, and {21.1} pole figures was analyzed with a DRON-7 X-ray texture diffractometer using Co$K\alpha$ radiation in reflection geometry. Tilt angle α and rotation angle β were varied in the ranges 0°–70° and 0°–360°, respectively, at a steps of 5°. The defocusing-induced decrease in the intensity at the periphery of pole figures was corrected using correction coefficients, in the calculation of which we took into consideration the conditions of X-ray recording of the pole figures. The set of texture components was selected from an analysis of orientation distribution function (ODF) sections calculated from experimental pole figures. A newly created file with orientations, which included three Euler angles and preliminary parameters W_i and ε_i (the volume fractions of the main orientations and the scattering parameter, respectively), was processed with the Texxor program [9].

Tensile tests were conducted according to GOST (State Standard) 11701–84 with an Instron-1185 testing machine at room temperature and a strain rate of 2×10^{-3} s^{-1}. Specimens 20 × 20 × 100 mm in dimensions were deformed by longitudinal extension at room temperature in a tensometer (with a gage size of 4.35 mm and scale of 25%) until necking, which was identified by a load fall after reaching the maximum load. The test results were used to estimate yield strength σ_y, ultimate tensile strength σ_u, strain-hardening coefficient *n*, and uniform relative elongation δ_u.

δ_u was calculated by the formula

$$n = \ln(1 + \delta_u).$$

The value of each mechanical property was determined by averaging the results of three measurements per point.

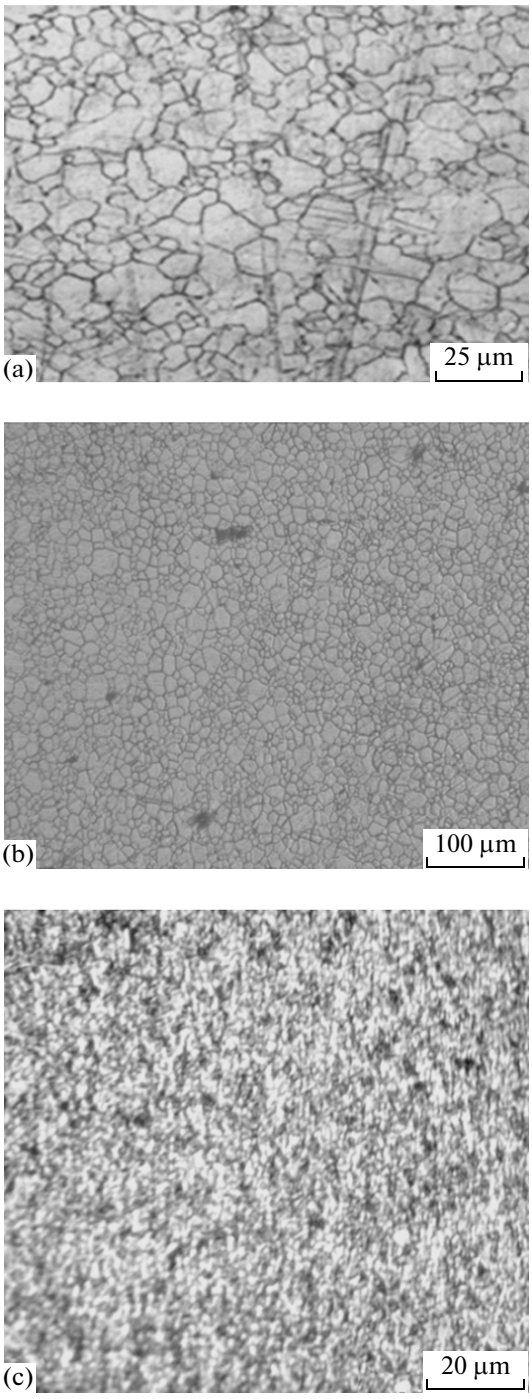

Fig. 1. Microstructure of the MA2-1hp alloy (a) in the initial state and after the (b) first and (c) second ECAP stage.

RESULTS AND DISCUSSION

Figure 1a shows the microstructure of the MA2-1hp alloy along the longitudinal direction of the initial extruded rod. The presence of quite coarse grains (>20 μm) together with finer ones characterizes the microstructure of the initial state. An average grain size is 12.4 μm.

After the first stage of ECAP by route 2*C* (two passes at 245°C) and subsequent annealing at 375°C for 1 h, the average grain size decreases to 9.4 μm (Fig. 1b). This ECAP stage with subsequent annealing is aimed at increasing the low-temperature ductility of the alloy and preparing samples to the second stage of severe plastic deformation, during which grain refinement proceeds until the grain size becomes difficult to measure with the same technique (Fig. 1c). Therefore, in this case we used TEM. Figure 2 shows a typical TEM image of the resultant microstructure and a grain size distribution histogram.

Many electron microscopy images of the structure exhibit distinct diffraction contrast of grains. The fringe contrast at grain boundaries indicates that they are high-angle boundaries. Electron microscopy images show both fine recrystallized and coarse grains. The coarse grains usually have high-angle equilibrium boundaries.

To be aware of the grain size, we analyzed 20 electron-microscopic images. Over 500 grains were measured to estimate the average size. The average grain size was 0.64 μm.

In an analysis of electron-microscopic images, we also revealed a new phase, the average maximum particle size of which was 0.24 μm. A large scatter of the phase particle sizes should be noted: from fine point-like to large ones that are similar to the fine grains in the matrix. In most cases, phase particles are round or oval. No strictly defined arrangement of the particles was observed: they were located both at boundaries and inside grains. It can be seen in some images that a phase particle retards the movement of a grain boundary (see Fig. 2a).

To determine the composition of the detected phase, XRD analysis of the spectra of samples in the initial alloy state and after two-stage ECAP was additionally carried out. Figure 3 shows X-ray diffraction patterns for the first lines (low 2θ angles) of the MA2-1hp alloy in these states.

In the initial state and after the first ECAP stage, only XRD peaks from the magnesium matrix are present. After the second stage, there are peaks corresponding to the $Mg_{17}Al_{12}$ phase (bcc lattice, a lattice parameter of 10.5438 Å; see Fig. 3c) along with those from the main phase of the alloy (solid solution). The volume fraction of the $Mg_{17}Al_{12}$ phase is 5.45%. The concentration of the particles of this phase in the alloy structure in the initial state and after the first ECAP stage seems to be less than 3%; therefore, no XRD peaks are observed in the X-ray diffraction patterns. An increase in the amount of precipitations after the

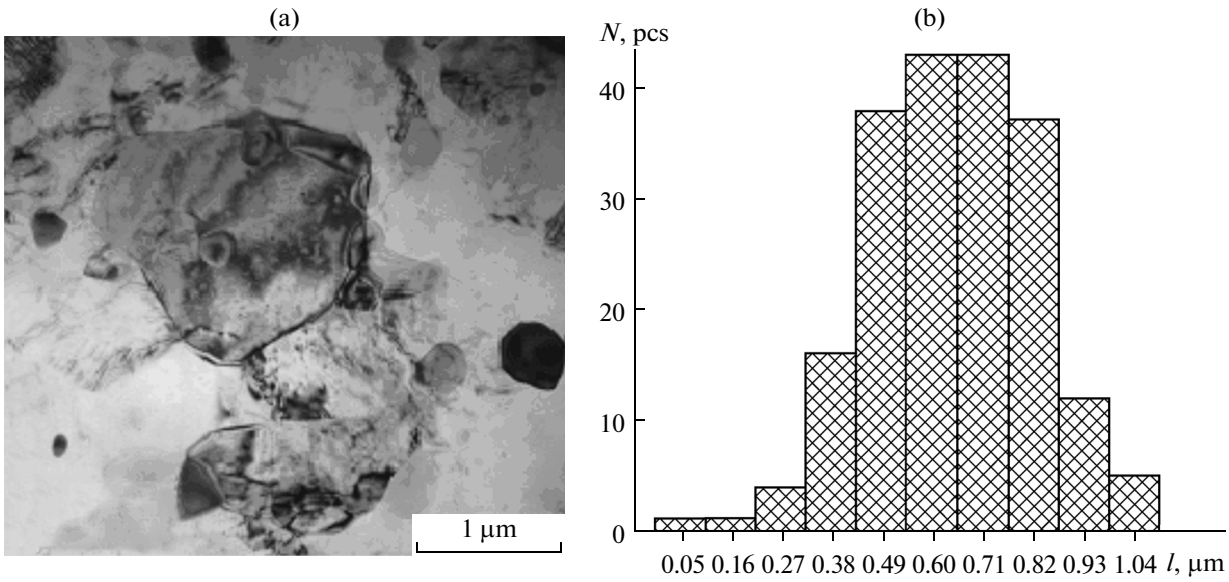

Fig. 2. TEM microstructure of the MA2-1hp alloy (a) after the second ECAP stage and (b) grain size distribution diagram (N is the number of grains and l is the length).

second ECAP stage can be explained by a decrease in the pressing temperature.

Figure 4 presents pole figures and ODF sections for the alloy in the initial state and after two stages of ECAP.

It is follows from the texture study that the initial texture of the alloy is characterized by a set of the main orientations that are typical of hot-pressed MA2-1hp alloy rods with predominant $\langle 10\bar{1}0\rangle$ and $\langle 11\bar{2}0\rangle$ directions, which are parallel to the pressing direction, at a total volume fraction of the orientations $W_\Sigma = 0.46$. After the first stage of ECAP with subsequent annealing, the alloy exhibits a texture that can be described as a scattered basal texture tilted at an angle of 43° to the pressing direction and having a maximum orientation density of 4.2. It is seen that the scattering increases as compared to the initial state. After the second ECAP stage, the alloy exhibits the same type of texture as after the first stage. There are the following differences: the angle of basal texture inclination to the pressing direction increases to 53°, and the maximum orientation density of the main orientation grows to 6.4. An increase in the texture sharpness results from a decreased pressing temperature, and an increase in the angle of the basal component results from an increased angle of channel intersection.

ECAP radically changed the texture due to active shear strains at an angle of 45° to the pressing direction. This change in the texture is also accompanied by a significant scattering of the main orientations. This fact is supported by high volume fractions of the textureless component. The volume fraction of the textureless component increases to 0.82 and 0.86 after both the first and the second ECAP stages, respectively.

Knowing the Eulerian angles and the volume fractions of orientations, we were able to estimate the generalized Schmid and orientation factors [6, 7] (Table 1).

Table 1. Orientation factors M_i for various deformation systems and alloy processing regimes

Sample	Processing regime*	Deformation system			
		basal	prismatic	pyramidal	twinning
1	Initial state	8.594	4.471	5.490	5.557
2	ECAP-2C + annealing	4.941	5.862	6.297	7.275
3	The same + ECAP-12ACB_c	4.878	5.961	6.455	7.752

* Numerals at the pressing routes indicate the number of passes.

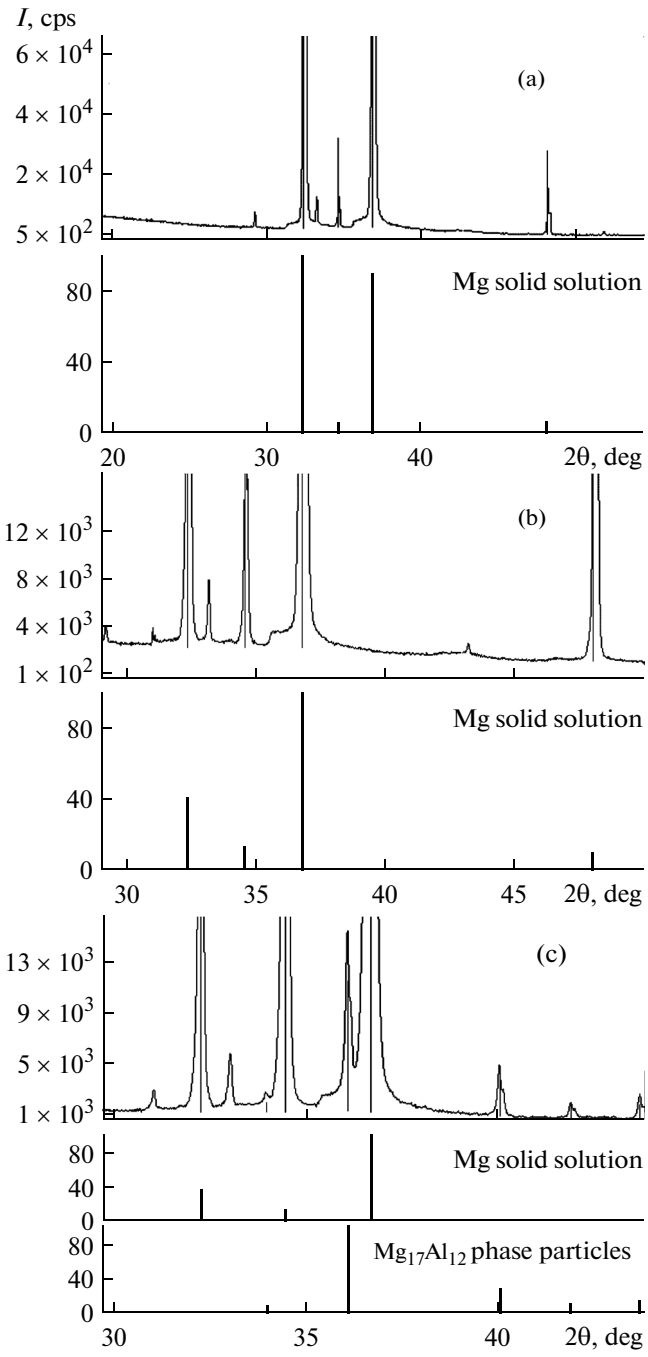

Fig. 3. X-ray diffraction pattern of the MA2-1hp alloy (a) in the initial state and after the (b) first and (c) second ECAP stages.

We can draw the conclusion from Table 1 that the activity of basal slip increases after ECAP (orientation factors for basal slip almost two times lower than those in the initial state), which should have a positive effect on the ductility of the alloy. The given orientation factors suggest that the activity of the remaining deformation systems varies only slightly during ECAP and subsequent annealing.

It is clear from a comparison of the resultant average grain sizes and the mechanical properties of the alloy in its different states (Table 2) that the minimum grain size (0.64 μm) was achieved after the second ECAP stage, unlike the initial-state values of the tensile strength (279 MPa) and the yield strength (220 MPa). Uniform elongation δ_u is maximal after the first stage of ECAP (44.2%) due to annealing after ECAP, whereas it decreases noticeably after the second stage (18%) but still almost two times higher than the similar value of the initial state.

These results can be explained using the Hall–Petch relation. According to Armstrong's theory for textured magnesium alloys [10], the Hall–Petch relation can be written as follows:

$$\sigma_y = M\tau_{bas} + kd^{-1/2},$$

where σ_y is the yield strength, M is the orientation factor for basal slip, τ_{bas} is the critical resolved shear stress (CRSS) for basal slip, k is a material constant, and d is the average grain size.

Data on the mechanical properties and the average grain size of the initial state satisfy the previously deduced Hall–Petch relation for magnesium alloys subjected to direct pressing [4],

$$\sigma_y = 140.8 + 350d^{-1/2}.$$

Table 2. Average grain size and mechanical properties of the MA2-1hp alloy after processing under experimental conditions

Sample	Processing regime*	d, μm	$d^{-1/2}$	$\sigma_{0.2}$	σ_u	δ_u, %
				MPa		
1	Initial state	12.4	284.0	220	279	10.2
2	ECAP-2C + annealing	9.4	326.2	91	236	44.2
3	The same + ECAP-12ACB_c	0.64	877.0	185	252	18.0

See the footnote to Table 1.

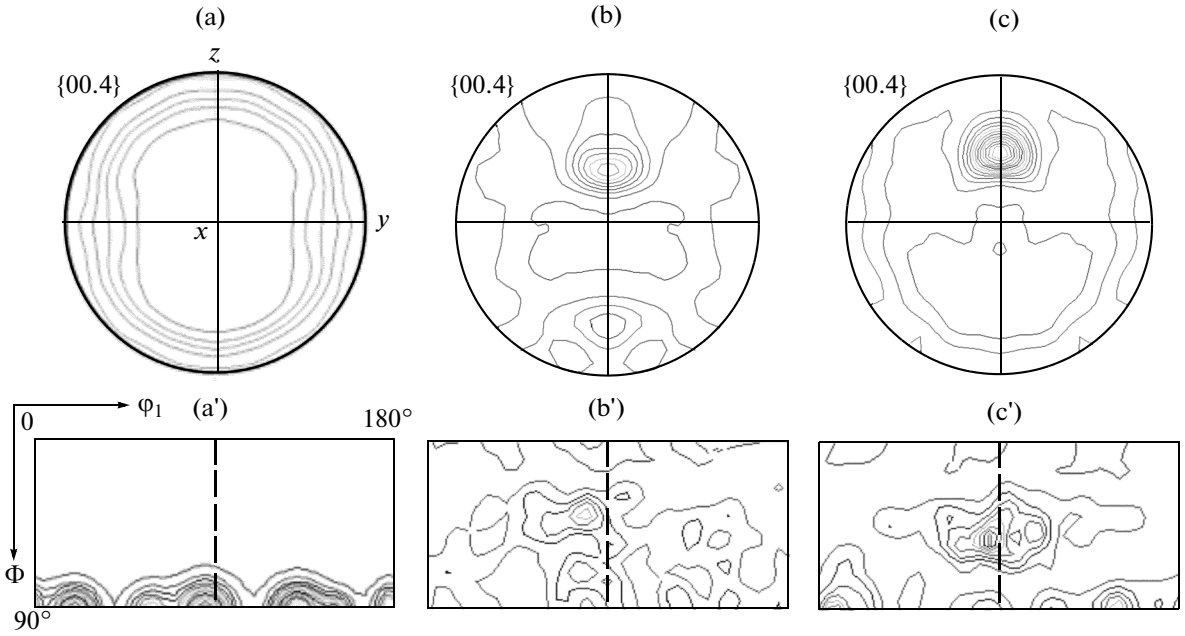

Fig. 4. (a–c) Pole figures and (a'–c') ODF sections at $\varphi_2 = 0°$ of the MA2-1hp alloy: (a, a') initial state; (b, b') after the first stage; and (c, c') after the second stage of ECAP.

Our results for the yield strength (MPa) and the average grain size (μm) for the first ECAP stage and subsequent annealing satisfy the previously derived Hall–Petch relation [6] (Fig. 5),

$$\sigma_y = 30.3 + 184.6d^{-1/2}. \quad (1)$$

Similar Hall–Petch equations were also derived in [3, 4]. It is seen that, after the second ECAP stage, the yield strength of the alloy satisfies the Hall–Petch relation derived earlier for magnesium with a submicrocrystalline grain size (1–0.1 μm) [11],

$$\sigma_y = 143.2 + 41.9d^{-1/2}. \quad (2)$$

A change in components σ_0 (increase) and k (decrease) was noticed in the case described by Eq. (2) as compared to Eq. (1) due to the additional activation (see data on the structure factor) of multiple slip and twinning at the expense of basal slip in this alloy.

The formation of such a submicrocrystalline structure in the alloy with an average grain size of 0.64 μm, which activates nonbasal slip systems, becomes possible due to the retardation of grain growth by $Mg_{17}Al_{12}$ particles.

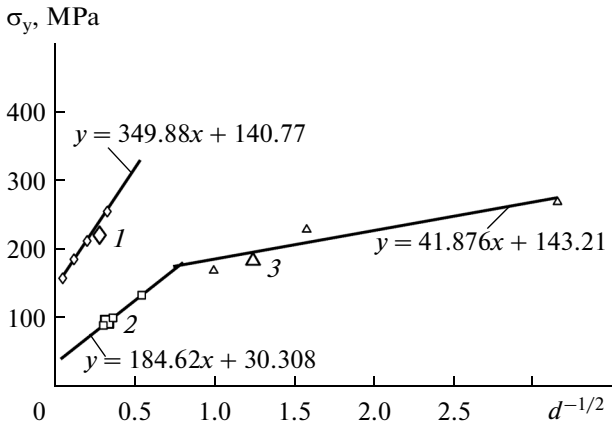

Fig. 5. Dependences $\sigma_y(d^{-1/2})$ and the corresponding linear Hall–Petch relations for MA2-1hp samples (*1*) in the initial state and (*2*) after ECAP (Tables 1, 2; regimes 2, 3).

CONCLUSIONS

(1) Two-stage ECAP at a deformation end temperature of 150°C resulted in the formation of a submicrocrystalline structure with an average grain size of 0.64 μm. The second stage of ECAP led to the formation of fine $Mg_{17}Al_{12}$ particles with an average size of 0.24 μm and a volume fraction of 5.45%.

(2) The basal texture of the alloy in the initial hot-pressed state after ECAP according to the chosen conditions transforms into a scattered basal one inclined at an angle of 39°–51° to the pressing direction.

(3) The first stage of ECAP and subsequent annealing maximally enhanced the alloy ductility, reaching a uniform relative elongation of 44% at a yield strength and a tensile strength of 91 and 236 MPa, respectively. The second ECAP stage caused alloy hardening (the yield strength and the tensile strength increased to

185 and 252 MPa, whereas the uniform relative elongation decreased to 18%).

(4) When explaining the results, we noted the effect of orientation and structural factors of the investigated alloy on the Hall–Petch coefficients.

ACKNOWLEDGMENTS

This work was supported by the Russian Foundation for Basic Research (project no. 11-03-00335-a).

REFERENCES

1. T. Mukai, M. Yamanoi, H. Watanabe, and K. Higashi, "Ductility enhancement in AZ31 magnesium alloy by controlling its grain structure," Scr. Mater. **45**, 89–94 (2001).
2. S. R. Agnew, J. A. Horton, T. M. Lillo, and D. W. Brown, "Enhanced ductility in strongly textured magnesium produced by equal channel angular pressing," Scr. Mater. **50**, 377–381 (2004).
3. Y. Yoshida, L. Cisar, S. Kamado, and Y. Kojima, "Effect of microstructural factors on tensile properties of an ECAE-processed AZ31 magnesium alloy," Mater. Trans. **44**, 468–475 (2003).
4. W. J. Kim and H. T. Jeong, "Grain-size strengthening in equal-channel-angular-pressing processed AZ31 Mg alloys with a constant texture," Mater. Trans. JIM **46**, 251–268 (2005).
5. V. N. Serebryany and S. V. Dobatkin, "The role of structure and texture factors in the ductility and deformability improving of magnesium alloys subjected to ECAP," Mater. Sci. Forum **702–703**, 119–122 (2012).
6. V. N. Serebryany, G. S. D'yakonov, V. I. Kopylov, G. A. Salishchev, and S.V. Dobatkin, "Texture and structure contribution to low-temperature plasticity enhancement of Mg–Al–Zn–Mn alloy MA2-1hp after ECAP and annealing," Phys. Met. Metallogr. **114** (5), 448–456 (2013).
7. V. N. Serebryany, T. M. Ivanova, V. I. Kopylov, S. V. Dobatkin, N. N. Pozdnyakova, V. A. Pimenov, and T. I. Savelova, "Effect of equal-channel angular pressing and annealing conditions on the texture, microstructure, and deformability of an MA2-1 alloy," Russian Metallurgy (Metally), No. 7, 592–602 (2010).
8. S. X. Ding, W. T. Lee, C. P. Chang, L. W. Chang, and P. W. Kao, "Improvement of strength of magnesium alloy processed by equal channel angular extrusion," Scr. Mater. **59**, 1006–1009 (2008).
9. S. F. Kurtasov, "Method for the quantitative analysis of rolling textures of materials with a cubic crystal lattice," Zavod. Lab. **73** (7), 29–36 (2007).
10. Rao G. Sambasiva and Y. V. R. K. Prasad, "Grain boundary strengthening in strongly textured magnesium produced by hot rolling," Metall. Trans. A **13**, 2219–2226 (1982).
11. H. J. Choi, Y. Kim, J. H. Shin, and D. H. Bae, "Deformation behavior of magnesium in the grain size spectrum from nano- to micrometer," Mater. Sci. Eng. A **527**, 1565–1570 (2010).

Translated by T. Gapontseva